Pattern formation during phase transitions: kinetics of partially conserved order parameters and the role of gradient energies

1994 J. Phys.: Condens. Matter 6 11027

(http://iopscience.iop.org/0953-8984/6/50/012)

J. Phys.: Condens. Matter 6 (1994) 11027–11034. Printed in the UK

Pattern formation during phase transitions: kinetics of partially conserved order parameters and the role of gradient energies

I Tsatskis†‖, E K H Salje†‡ and Volker Heine§

† Department of Earth Sciences, Downing Street, Cambridge CB2 3EQ, UK

‡ Interdisciplinary Research Centre in Superconductivity, Madingley Road, Cambridge CB3 0HE, UK

§ TCM, Cavendish Laboratory, Madingley Road, Cambridge CB2 0HE, UK

Received 14 March 1994, in final form 3 October 1994

Abstract. The formation of kinetic, transient microstructures in structural phase transitions is analysed within the framework of time-dependent Landau–Ginzburg theories. The mesoscopic rate equation is $\partial\phi/\partial t = \phi - \phi^3 + \partial^2\phi/\partial x^2 - \gamma\,\partial^2\phi/\partial x^4 + \delta\,\partial^6\phi/\partial x^6$. A front of a stable state $\phi = 1$ can grow into an unstable region with $\phi = 0$ in an oscillatory manner. It will then leave behind a transient domain structure with quasi-periodic walls. Such domain structures occur for positive and negative values of γ with sufficiently large values of $|\gamma|$. The phase diagram in (γ, δ) space is explored using computer simulation. The repetition length does not diverge at the bifurcation between an oscillatory and solitonic regime except at the point $\gamma = 1/12$, $\delta = 0$ studied previously. It is shown that recent computer simulation studies of 'realistic' microstructures used implicit values of γ and δ close to the bifurcation condition.

1. Introduction

Structural phase transitions can generate patterns of microdomains for a sufficiently rapid quench through the transition temperature T_c. The most commonly observed patterns for $T < T_c$ are somewhat periodic arrays of twin walls (the 'stripe' pattern) and interwoven wall segments (the 'tweed' pattern). Nearly every framework structure with atomic ordering strongly coupled with strains (e.g., ferroelastic and co-elastic crystals) show such patterns under suitable conditions for rapid change of temperature or pressure [1]. Typical examples are the oxygen–vacancy ordering in $YBa_2Cu_3O_7$ superconductor [2, 3], Al–Si ordering in feldspars and cordierites [4, 5, 6] and the ferroelastic transitions in Ba-doped $Pb_3(PO_4)_2$ [7]. In all of these cases the patterns are thermodynamically unstable inhomogeneous structures although they persist for long times (even geological times for feldspars [4, 5]).

The same pattern formation is also observed in generic computer experiments when pseudo-spin coordinates are indirectly coupled via elastic forces [8–13]. Such models invariably show tweed as the first kinetic microstructure which often develops under annealing into a stripe pattern. Both the direct observation and the computer experiment show that the length scale of the pattern is mesoscopic, i.e. it extends from some 10 Å to several hundred ångströms. Furthermore, these mesoscopic structures are very similar in many different materials. We may assume, therefore, that we are dealing with an universal

‖ Previous name: I V Masanskii.

0953-8984/94/5011027+08$19.50

phenomenon in many (if not all) ferroelastic and co-elastic phase transitions with sufficiently long transient times.

Kinetic microstructures are firmly established, therefore, both from experimental observations and generic computer experiments. Their analytical description, on the other hand, is far from being clear. The probably most promising attempt to formulate an analytical theory was based on the following idea [14–17]. Consider a sample cooled quickly through the transition temperature and let precursor ordering occur in part of the sample (e.g. due to surface relaxations [18, 19]. The kinetic process may then, at least partly, relate to the growth of such a nucleus. Due to the anisotropic nature of the elastic interactions, walls can only be generated parallel to one of two well-defined planes with normals which are usually referred to as 'soft' directions [1]. Any movement of a wall maintains its orientation, so rotations and bending of walls do not occur in the defect-free crystal with only one wall orientation present. Arrays of walls with the same orientation form stripe patterns. Here we attempt to describe such stripe patterns in a simple 1D picture. The fundamental question is now: how does the boundary between the stable and unstable state of the material move through the sample when a crystal is cooled through a phase transition. We show in this paper that solitary kink movements exist only under rather limiting physical conditions whereas oscillatory movements are rather common solutions. This result may shed some light on the experimental observation that periodic (or nearly so) stripe patterns are often observed in ferroelastics where lateral movements of walls after their generation virtually never takes place in a stress-free material [1]. It is very likely, therefore, that the stripe pattern is the result of the kinetic transformation of the high-symmetry phase into the low-symmetry phase, e.g. in a quench experiment, and is not due to a reshuffle of pre-existing domain walls. How far our approach is realistic depends largely on the appearance of the tweed microstructure as a precursor of the stripe pattern (e.g. in $YBa_2Cu_3O_7$ [2, 3] and cordierite [4]). In ferroelastic materials such as $Pb_3(PO_4)_2$ stripe patterns appear without prior tweed formation and it is likely that our present approach may be applicable for these materials [1, 7, 20].

Stripe patterns as the result of the kinetic phase transitions after rapid undercooling were already postulated as the solution of a general rate equation of partially conserved order parameters [14]. The driving force for the kinetic process was related to an excess Gibbs free energy of the phase transition of Landau–Ginzburg type with a second-order gradient energy. In this paper we generalize the approach and explore the conditions for pattern formation for kinetic rate equations with driving forces including second-, fourth- and sixth-order gradient terms. We show that sufficiently large positive or negative fourth-order gradient terms lead to pattern formation whereas large positive sixth-order terms stabilize solitary kink waves.

2. The rate equation

We start from the rate equation discussed in detail [14] with an order parameter Q which is essentially non-conserved with possible weak contributions from local conservation. The driving force is related to the excess Gibbs free energy G of the phase transition [1, 14] and the corresponding rate equation [20–22] is

$$\frac{\partial Q}{\partial t} = -\frac{1}{\tau}\left(1 - \frac{\xi_c^2}{\xi^2}\frac{\sinh(\xi\nabla)}{\xi\nabla}\right)\frac{\delta G}{\delta Q} \tag{1}$$

where ξ, ξ_c are lengths related to the conservation behaviour of the order parameter with

$$G = \int \mathrm{d}\vec{r}\left[\frac{1}{2}aQ^2 + \frac{1}{4}bQ^4 + \frac{1}{2}g|\nabla Q|^2 + \frac{1}{2}h\left(\nabla^2 Q\right)^2\right]. \tag{2}$$

The bracket in equation (1) contains gradient operators in the kinetic prefactor; its application is to be understood in the usual way as a series expansion in the gradient operator [22].

Consider first a fully non-conserved ordering process. Assuming changes of the order parameter only in one direction (e.g., x), we have

$$\tau\frac{\partial Q}{\partial t} = |a|Q - bQ^3 + g\frac{\partial^2 Q}{\partial x^2} - h\frac{\partial^4 Q}{\partial x^4}. \tag{3}$$

Weak conservation modifies the equation coefficients in a following way:

$$\begin{aligned} a \to a' &= a\left(1 - \frac{\xi_c^2}{\xi^2}\right) \qquad b \to b' = b\left(1 - \frac{\xi_c^2}{\xi^2}\right) \\ g \to g' &= g\left(1 - \frac{\xi_c^2}{\xi^2}\right) - \frac{1}{6}\xi_c^2|a| \qquad h \to h' = h\left(1 - \frac{\xi_c^2}{\xi^2}\right) + \frac{1}{6}\xi_c^2 g + \frac{1}{120}\xi_c^2\xi^2|a|. \end{aligned} \tag{4}$$

Rescaling the time, spatial coordinate, and order parameter

$$t' = \frac{|a'|}{\tau}t \qquad x' = \sqrt{\frac{|a'|}{g'}}x \qquad \phi = \frac{Q}{Q_0} \qquad Q_0 = \sqrt{\frac{|a'|}{b'}} \tag{5}$$

leads to the rate law in dimensionless parameters:

$$\frac{\partial\phi}{\partial t'} = \phi - \phi^3 + \frac{\partial^2\phi}{\partial x'^2} - \gamma\frac{\partial^4\phi}{\partial x'^4} \tag{6}$$

which is the so-called extended Fisher–Kolmogorov (EFK) equation [15, 16], with

$$\gamma = h'|a'|/g'^2. \tag{7}$$

In the case of absence of both conservation ($\xi_c = 0$) and a higher-order gradient term ($h = 0$) in the expression for the free energy, we have $\gamma = 0$, and this corresponds to the case of the ordinary (non-extended) Fisher–Kolmogorov (FK) equation [17]. Weak conservation with $h = 0$ corresponds to positive values of γ, while in the non-conserved regime h can be negative leading to $\gamma < 0$. This means that the coefficient γ in the EFK equation can be both positive and negative. In the case where $\gamma < 0$ the model is unstable at short wavelengths and the EFK equation must be extended further to include the sixth-order derivative with positive coefficient δ in order to find stable solutions:

$$\frac{\partial\phi}{\partial t'} = \phi - \phi^3 + \frac{\partial^2\phi}{\partial x'^2} - \gamma\frac{\partial^4\phi}{\partial x'^4} + \delta\frac{\partial^6\phi}{\partial x'^6}. \tag{8}$$

A sixth-order term also follows, of course, from the mixing of second- and fourth-order terms in the kinetic prefactor and the derivative of the Gibbs free energy. In all cases we arrive at the same equation (8). We will now analyse the solutions of this equation for the initial conditions described in the introduction, i.e. a region with $\phi = 1$ growing with a front into a region of $\phi = 0$.

3. Pattern formation

The following question now arises: under which condition does pattern formation occur? Furthermore, we ask what the geometrical nature of the front propagation is. It is an object of the present work to study the pattern formation for equation (8) on the half-plane (γ, $\delta > 0$). Previous research focused on the simple case $\gamma > 0$, $\delta = 0$ [14, 15], where a bifurcation was found for $\gamma = \gamma_c = 1/12$ with pattern formation for $\gamma > \gamma_c$, its absence for $\gamma < \gamma_c$, and diverging repetition length λ for $\gamma \to \gamma_c$. Using the language of phase transitions, this bifurcation has qualities of a second-order behaviour (with λ playing the role of a correlation length).

In order to explore the bifurcation behaviour in the (γ, δ) space, we have undertaken numerical simulation of our equation. The starting condition was always a nucleus of the stable phase $\phi = 1$ with a front of the shape $\exp(-x^2/a^2)$ with $a = 4$ growing into the unstable state $\phi = 0$. The time evolution of ϕ was then calculated by solving equation (8) numerically using a standard FTCS (forward-time–centred-space) finite-difference representation method [30]. The step size in space was 0.05 and in time space 0.001; further tests did not show any dependence on the step size. We used fixed boundary conditions. Tests with different sample sizes (>500) did not indicate finite-size effects in the intervals shown in figure 1.

In all calculations, we find that the unstable state $\phi = 0$ transforms to the stable state $\phi = 1$. This corresponds to a simple propagation of the front. After some time steps this propagation changes for sufficiently large values of $|\gamma|$. The front inverts the stable state $\phi = 1$ into the equally stable state $\phi = -1$ leaving behind a kink. This process is then, after some more time steps, inverted and produces an antikink. The distance between kinks and antikinks is constant after the first few oscillations and we refer to this distance as the repetition length. The generation of kinks and antikinks continues until the entire regime $\phi = 0$ is transformed into a pattern with domains of $\phi = 1$ and $\phi = -1$.

The numerical solutions are shown in figure 1. The detailed analysis shows two types of pattern. In each case a bifurcation point was found with γ_c increasing with δ_c. The first type relates to solutions with $\gamma > 0$. The inverse repetition length does not disappear for $\delta > 0$; instead, it jumps from zero to some finite value. In this sense, this behaviour could be called 'first order'. For $\delta = 0$ the repetition lengths were found to be the same as calculated using the analytical method discussed in [15].

The second type of pattern formation occurs for $\gamma < 0$. Bifurcation was observed approximately along the line $\delta = -\gamma^2/3$. There is no divergence of the repetition length. The difference from the pattern corresponding to positive γ is that the propagation front always shows precursor 'ripples'. These ripples were predicted from atomistic calculations [18, 19] and its has been suspected that they occur in ferroelastic $Pb_3(PO_4)_2$ [7].

Let us now turn to the phase diagram for the solitonic and oscillatory solutions to our equation. Such a phase diagram was derived from numerical calculations and is shown in figure 2. For small values of δ it shows a narrow gap between two regions with pattern formation. Inside the gap we find only solitonic movements. This gap extends from $\gamma = 0$ to $\gamma = 1/12$. The surprising result is, thus, that for small δ, pattern formation almost always occurs, notably for both positive *and* negative γ. The role of δ is to increase the gap, i.e. the sixth-order gradient of term reduces the tendency of the front propagation to oscillate. This effect is very large; with $\delta = 0.1$, we find that the gap now extends from $\gamma = -0.55$ to $\gamma = 0.3$, i.e. the sixth-order gradient term efficiently stabilizes the solitonic movement and prevents pattern formation. Note that in the $\gamma < 0$ regime the model becomes unstable as δ goes to zero; this means that the line $\gamma < 0$, $\delta = 0$ is not included in the phase diagram.

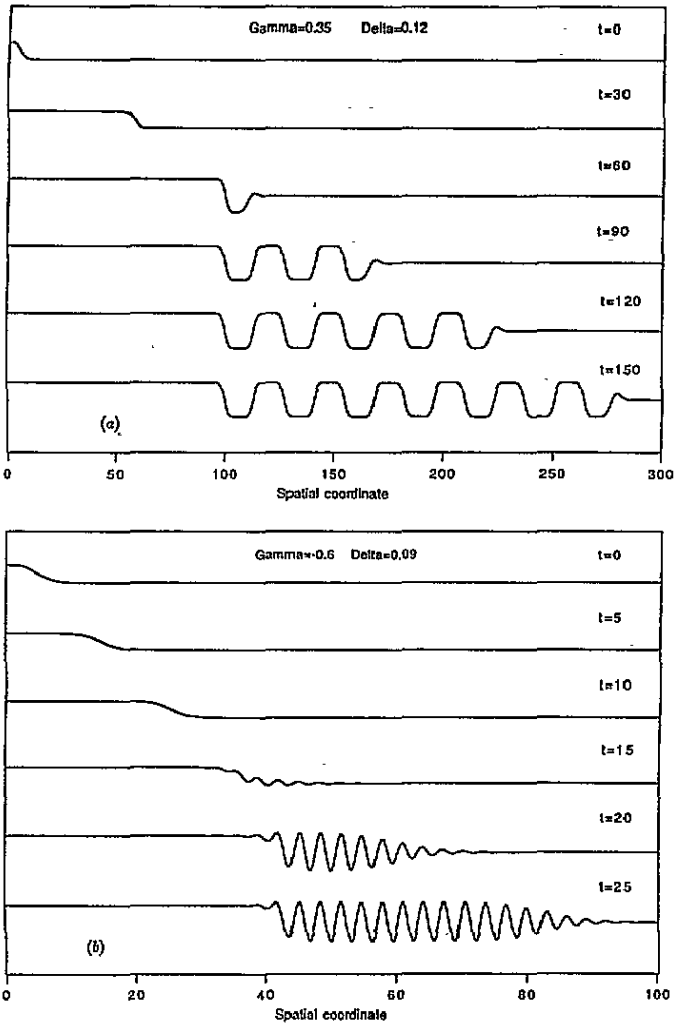

Figure 1. Profiles of a propagating front at different times for (a) positive and (b) negative values of γ. The stable state grows into the area of the unstable state and reverts from order ($\phi = 1$) to anti-order ($\phi = -1$) after some initial propagation. Oscillatory behaviour follows in both cases leaving an unstable (but long-lived) pattern behind the propagation front. The main difference between (a) and (b) is the formation of precursor ripples [18] for $\gamma < 0$ but not for $\gamma > 0$.

Finally, we compare our results with those of recent computer simulations of the microstructures in high-temperature superconductors [9–11] and related general models [23, 24]. In these models, no partial conservation is taken into consideration (i.e. $\xi_c = 0$). The higher-order gradient terms stem now from the way local state parameters interact via lattice distortions. It was found that stripe patterns always develop along specific directions (the so-called 'soft' directions {110} in $YBa_2Cu_3O_7$).

Consider mapping of the effective Ising model for this situation onto the equation studied above. The strain-mediated interaction allows treatment in the framework of mean-field theory [8, 25, 26]. We will use the expression for the free energy in this approximation [27]

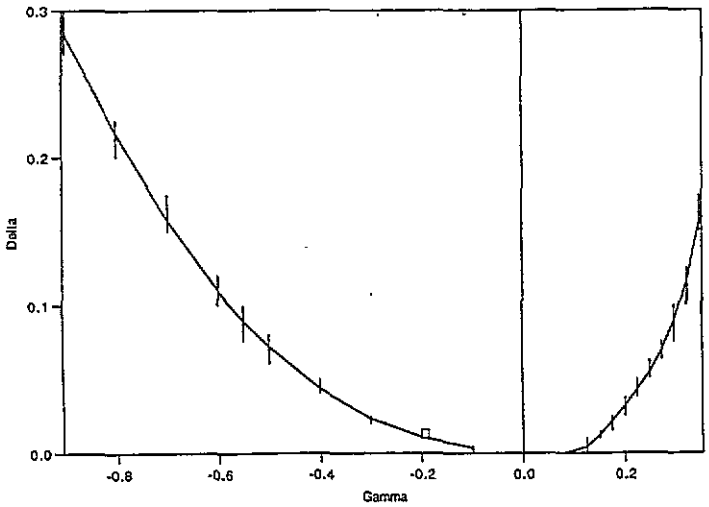

Figure 2. A phase diagram for pattern formation on the half-plane (γ, $\delta > 0$). Two branches corresponding to different signs of γ constitute a boundary which separates oscillatory and solitonic movement of the front. The areas below and above the boundary correspond to the presence and absence of pattern, respectively. The rectangle corresponds to the values of γ and δ derived from parameters of the computer simulation (equation (16)).

$$G = E - TS \tag{9}$$

$$E = \frac{1}{2}\sum_{ij} J_{ij} Q_i Q_j \tag{10}$$

$$S = -\sum_i \left[\frac{1}{2}(1+Q_i)\ln\left(\frac{1}{2}(1+Q_i)\right) + \frac{1}{2}(1-Q_i)\ln\left(\frac{1}{2}(1-Q_i)\right)\right] \tag{11}$$

assuming that it is valid for arbitrary non-equilibrium order parameter distribution [28, 29]. Choosing a single direction for the pattern formation in the continuum limit (i.e. $Q(x, y, z)$ becomes $Q(x)$), we have for the internal energy

$$E = -\frac{1}{2}\sum_{k_x} J(k_x, 0, 0)|Q(k_x)|^2 \tag{12}$$

where $J(k)$ is determined by the strain-mediated interactions between spins including its specific k-dependence [23]. The wavevector expansion of $J(k_x, 0, 0)$ in the sixth order is

$$J(k_x, 0, 0) = (0, 0, 0) - gk_x^2 - hk_x^4 - pk_x^6 \tag{13}$$

where positive coefficients always lad to bell-shaped profiles. If h and/or p is negative but sufficiently small the bell shape is preserved. After conversion of the internal energy expression to direct space, and fourth-order expansion of the entropy in terms of the order parameter (sufficient to keep basic non-linearity), one again obtains the Ginzburg–Landau functional for the free energy. Rescaling the kinetic equation as before, we find the equation under study with the coefficients

$$\gamma = h|a|/g^2 \qquad \delta = p|a|^2/g^3 \tag{14}$$

where

$$a = T - J(0, 0, 0). \tag{15}$$

We now calculate γ and δ from the model parameters used in the computer experiment [23, 24] and find

$$\gamma = -0.193 \pm 0.007 \qquad \delta = 0.013 \pm 0.003. \tag{16}$$

This point lies on the bifurcation line within the accuracy of calculation (see figure 2). It appears to be likely, therefore, that a very stable stripe pattern observed in the atomistic computer simulation would also appear if a stable phase were to grow into the region of an unstable phase.

The fact that pattern formation from front propagation occurs for the same set of parameters for the Gibbs free energy as was used for an atomistic Hamiltonian in the computer simulation of microstructures from random noise may not be purely coincidental. In fact, the observed long lifetime of stripe patterns in the computer simulation might well relate to our result that similar patterns also emerge from front propagation. This conjecture can now be tested: if we change $J(k_x, 0, 0)$ in such a way that $\gamma = h|a|/g^2$ varies through the three stability fields in the phase diagram in figure 2, we expect extensive microstructures for large negative values of γ, more uniform structures inside the gap around $\gamma = 0$ and strong microstructures again for large positive values of γ. Computer simulation studies to test this hypothesis are planned.

References

[1] Salje E K H 1993 *Phase Transitions in Ferroelastic and Co-elastic Crystals* (Cambridge: Cambridge University Press)
[2] Schmahl W W, Putnis A, Salje E, Freeman P, Graeme-Barber A, Jones R, Singh K K, Blunt J, Edwards P P, Loram J and Mirza K 1989 *Phil. Mag. Lett.* **60** 241
[3] Krekels T, Van Tendeloo G, Broddin D, Amelinckx S, Tanner L, Mehbod M, Vanlanthem E and Deltour R 1991 *Physica* C **173** 361
[4] Putnis A, Salje E, Redfern S A T, Fyfe C A and Stroble H 1987 *Phys. Chem. Mineral.* **14** 446
[5] Wruck B, Salje E and Graeme-Barber A 1991 *Phys. Chem. Mineral.* **17** 700
[6] Putnis A and Salje E K H 1994 *Phase Transitions* **48** 85
[7] Bismayer U, Hensler J, Salje E K H and Güttler B 1994 *Phase Transitions* at press
[8] Marais S, Heine V, Nex C and Salje E 1991 *Phys. Rev. Lett.* **66** 2480
[9] Parlinski K, Heine V and Salje E K H 1993 *J. Phys.: Condens. Matter* **5** 497
[10] Parlinski K, Salje E K H and Heine V 1993 *Acta Metall. Mater.* **41** 839
[11] Bratkovsky A M, Salje E K H, Marais S C and Heine V 1994 *Phase Transitions* **48** 1
[12] Marais S C, Salje E K H, Heine V and Bratkovsky A M 1994 *Phase Transitions* **48** 15
[13] Semenovskaya S and Khachaturyan A G 1991 *Phys. Rev. Lett.* **67** 2223
[14] Salje E K H 1993 *J. Phys.: Condens. Matter* **3** 3667
[15] Dee G T and van Saarloos W 1988 *Phys. Rev. Lett.* **60** 2641
[16] van Saarloos W 1987 *Phys. Rev. Lett.* **58** 2571
[17] Aronson D G and Weinberger H F 1978 *Adv. Math.* **30** 33
[18] Houchmanzadeh B, Lajzerowicz J and Salje E 1992 *Phase Transitions* **38** 77
[19] Houchmanzadeh B, Lajzerowicz J and Salje E 1992 *J. Phys.: Condens. Matter* **4** 9779
[20] Salje E K H, Wruck B, Graeme-Barber A and Caprenmter M A 1993 *J. Phys.: Condens. Matter* **5** 2961
[21] Salje E K H and Kroll H 1990 *Phys. Chem. Mineral.* **17** 563
[22] Marais S and Salje E 1991 *J. Phys.: Condens. Matter* **3** 3667
[23] Bratkovsky A M, Marais S C, Heine V and Salje E K H 1993 *J. Phys.: Condens. Matter* **6** 3679
[24] Bratkovsky A M, Salje E K H, Marais S C and Heine V 1993 *Phys. Rev.* submitted

[25] Salje E K H 1992 *Phys. Rep.* **215** 49
[26] Cowley R A 1976 *Phys. Rev.* B **13** 4877
[27] See, for example,
Brout R 1965 Phase Transitions (New York, Benjamin)
[28] Dattagupta S, Heine V, Marais S and Salje E 1991 *J. Phys.: Condens. Matter* **3** 2963
[29] Dattagupta S, Heine V, Marais S and Salje E 1991 *J. Phys.: Condens. Matter* **3** 2975
[30] Press W H, Flannery B P, Teukolsky S A and Vetterling W T 1986 *Numerical Recipes* (Cambridge: Cambridge University Press)